Development of thermosensitive chitosan/glicerophospate injectable in situ gelling solutions for potential application in intraoperative fluorescence imaging and local therapy of hepatocellular carcinoma: a preliminary study




# Development of thermosensitive chitosan/glicerophospate injectable in situ gelling solutions for potential application in intraoperative fluorescence imaging and local therapy of hepatocellular carcinoma: a preliminary study

| | |
|---|---|
| Journal: | *Expert Opinion on Drug Delivery* |
| Manuscript ID: | EODD-2015-0040.R1 |
| Manuscript Type: | Original Research |
| Keywords: | stimuli-sensitive hydrogel, chitosan, glycerophosphate, hepatocellular carcinoma, transarterial embolization, indocyanine green |
| | |

# Development of thermosensitive chitosan/glicerophospate injectable in situ gelling solutions for potential application in intraoperative fluorescence imaging and local therapy of hepatocellular carcinoma: a preliminary study


## Abstract

**Objectives:** Thermosensitive chitosan/glycerophosphate (C/GP) solutions exhibiting sol-gel transition around body temperature were prepared to develop a class of injectable hydrogel platforms for the imaging and loco-regional treatment of hepatocellular carcinoma (HCC). Indocyanine green (ICG) was loaded in the thermosensitive solutions in order to assess their potential for the detection of tumor nodules by fluorescence.

**Methods:** The gel formation of these formulations as well as their gelling time, injectability, compactness and resistance of gel structure, gelling temperature, storage conditions, biodegradability, in vitro dye release behavior were investigated. Ex vivo studies were carried out for a preliminary evaluation by using an isolated bovine liver.

**Results:** Gel strengths and gelation rates increased with the cross-link density between C and GP. These behaviors are more evident for C/GP solutions which displayed a gel-like precipitation at 4°C. Furthermore, formulations with the lowest cross-link density between C and GP exhibited the best injectability due to a lower resistance to flow. The loading of the dye did not influence gelation rate. ICG was not released from the hydrogels because of a strong electrostatic interaction between C and ICG. Ex vivo preliminary studies revealed that these injectable formulations remain in correspondence of the injected site.

**Conclusions:** The developed ICG-loaded hydrogels has the potential for intraoperative fluorescence imaging and local therapy of HCC as embolic agents. They form in situ compact gels and have a good potential for filling vessels and/or body cavities.

**Keywords**

Stimuli-sensitive hydrogel, chitosan, glycerophosphate, hepatocellular carcinoma, transarterial embolization, indocyanine green.

**Abbreviations:** EDTA ethylenediaminetetraacetic acid; HCC hepatocellular carcinoma; TAE transarterial embolization; TACE transarterial chemoembolization; C chitosan; GP glycerophosphate; C/GP chitosan/glycerophosphate; ICG indocyanine green; PBS Phosphate Buffer Saline; PDE Photo Dynamic Eye; LED light emitting diode , ω angular frequency; tan(δ) damping factor; G' storage modulus, G'' loss modulus

## 1. Introduction

Hepatocellular carcinoma (HCC) is an important cause of cancer deaths: each year more than 600,000 people die from HCC in the world [1].The hepatic resection represents the initial treatment for localized HCCs in patients without vascular invasion and with preserved hepatic functions [2]: the precise imaging of HCC nodules is clearly important for the success of the surgical procedure.

HCC is classified as a highly chemoresistant disease and conventional systemic chemotherapy plays almost no role in the treatment of advanced HCCs. For these reasons, localized anticancer therapies must be taken into account [3]. Among several locoregional ablative methods, transarterial embolization (TAE) consists of embolization of the artery feeding the tumor, which results in ischemia and subsequent tumor necrosis, while transarterial chemoembolization (TACE) implies the localized delivery of chemotherapeutic drugs combined with the use of embolic materials. The rationale is based on the fact that normal liver tissue receives its blood supply from the portal vein, whereas liver tumors mostly from the hepatic artery [4,5]: a combination of concentrated chemotherapy and local ischemia within the tumor can be synergistic in achieving tumor necrosis [6].

Nowadays, microparticles are used both as embolic agents (TAE), and as embolic drug carriers (TACE). In humans microparticles of size larger than 10 μm are used considering that capillary diameter is about 6-8 μm. Diameters from 40 to almost 1000 μm are suitable. Particles greater than 1000 μm can determine catheter clogging during the intra-arterial administration [3].

The microparticles can be classified as non-biodegradable (for example polyvinyl-alcohol (PVA) microspheres) or biodegradable (for example microspheres based on natural polymers such as starch, gelatin, chitosan or on synthetic polymers such as polylactic-co-glycolic acid (PLGA). Commercial products are available constituted by calibrated microspheres (drug empty particles to be loaded before use) that have changed the conditions of embolization: radiologists can adapt the size of microspheres to the size of the vessels to be occluded, in such a way to obtain an accurate targeting [7]. Several agents can be used for hepatic embolization; they have been recently reviewed [8]. Briefly, there are microspheres available on the market for so called "bland" embolization or transarterial embolization (TAE). These include Bead Block®, Embospheres®, Embozene® and Contour SE®. DC Bead® was designed to load therapeutic agents to enable one-step transarterial chemoembolization (TACE) and consists of polyvinyl alcohol (PVA) hydrogel modified with sulfonate groups that were first to demonstrate the ability to load and release chemotherapeutics in a controlled manner- a concept known as a drug-eluting bead (DEB). Other DEB systems are also now commercially available but based on microspheres with carboxylic acid functionality instead (HepaSphere® and Tandem®). All these commercial products are quite successful in the clinic, even if the intra-arterial local administration of microparticles can present some difficulties (such as catheter clogging). There is therefore the need of new embolizing systems, possibly not based on the intra-arterial administration of particles.

ICG is a water-soluble, amphiphilic tricarbocyanine dye that has a broad range of clinical applications due to its low toxicity and capacity to absorb and emit in the near-infrared spectral range [10]. Human tissue has the lowest absorption coefficient in the near-infrared part of the spectrum, therefore this dye is utilized for diagnostic and therapeutic applications.

Recent studies report the usefulness of ICG based intraoperative fluorescence imaging for the detection of HCC nodules. HCC tumors show very strong fluorescent signals in patients who had been given a ICG bolus several days before surgery as a routine preoperative liver function test [11-14]. The real mechanisms that mediate the preferential accumulation of ICG in HCC nodules instead of the normal liver tissue are still unknown. A hypothesis could be that ICG accumulates in regions of tissue possessing leaky capillaries of vessels [15] or disturbance of bile secretion [11].

As reported in literature [11,12,16], fluorescent nodules can be examined by a near infrared camera system named PDE (Photo Dynamic Eye, Hamamatsu Photonics K.K. Hamamatsu, Japan), that activates ICG with emitted light at a wavelength of 760 nm and filters out light with a wavelength below 820nm [17]. The light source is a light emitting diode (LED), and the detector is a charge-coupled device (CCD) camera. The camera unit of the device is directly handled and real-time fluorescence images can be observed on the monitor in the operating room. Thus, either nodules detection or hepatic resection could be performed under the guide of the PDE.

“Smart” hydrogels are constituted by polymer solutions which exhibit sol-gel phase transition in response to environmental stimuli such as pH, temperature, ionic strength, electric field, magnetic fields [18].

In situ thermo-sensitive hydrogels use temperature as the trigger of the gelation. Hence, it is possible to obtain hydrogels that are solutions at room temperature, but under physiological conditions (i.e., the body temperature) they form gels [19]. They can be designed as fluids that can be introduced into the desired tissue, organ or body cavity by simple syringe injection.

The viscosity of solutions can be low enough to allow direct blood administration. Thus after intra-arterial injection the solutions quickly form a gelled structure able to embolize the tumor [8,20] and to deliver imaging agents and/or drugs (if loaded in the precursor solution) [21]. Chitosan (C) is a cationic polysaccharide obtained by partial N-deacetylation of chitin. This polymer is widely used in the field of controlled drug release for its gelling properties, biodegradability and high biocompatibility [22-24].

The major issue concerning the applicability of C formulations is the impossibility of maintaining C in solution up to physiological pH due to its pKa (about 6.3). Above pH 6, C has no charge and it forms a gel-like precipitate [25].

Chenite and co-workers [25] developed a thermosensitive neutral aqueous solution based on C and glycerophosphate (GP) which exhibit sol-gel transition around body temperature. The addition of polyol salts, such as GP, leads to the transformation of pH-dependent C solutions into thermally sensitive pH-dependent solutions. In the presence of GP, C solutions remain liquid below room temperature, even with pH values within a physiologically acceptable neutral range from 6.8 to 7.2 [25]. These nearly neutral C/GP aqueous solutions gel when heated [26]. The neutralization behavior of GP determines C/GP solubility and phase transition phenomena. GP presents a mild alkalinity (pKa about 6.34) providing correct buffering without inducing immediate precipitation or gelation when the temperature provided is between 4 and 15ºC [26].

Taking into account these considerations, the aim of this work was the design and preparation of polymeric platforms based on C/GP and loaded with indocyanine green that might be used in the field of transarterial embolization and following intraoperative fluorescence imaging of HCC.

## 2. Experimental methods

### 2.1 Materials

Chitosan (C) was obtained from Primex ehf (Oslo, Norway). The deacetylation degree was 94% and the molecular weight was 103 kDa. Glycerophosphate (GP), hydrated disodic salt, was purchased from Sigma Aldrich (St. Louis, USA). Indocyanine Green (ICG) Pulsion was obtained from SEDA (Trezzano, Italy). The molecular weight was 774.96 Da. All other chemicals were of analytical grade.

### 2.2 Preparation of C/GP blank solutions

C/GP blank solutions at different concentrations (Table 1) were prepared according to the method of Kashyap and co-workers [27].

C was dissolved in 18 mL HCl 0.1 N and GP was solubilized in 2 mL of bidistilled water, at room temperature. The two solutions were put into an ice bath until the temperature of 4ºC was reached. Thereafter, GP solution was dropwise added, under vigorous magnetic stirring, into the C solution. The final solution was then left under stirring into the ice bath for 15 min, at 4°C. As reported in literature, in order to obtain liquid C/GP systems below room temperature a pH range of 6.8-7.2 is required [25]. For this reason the pH of all solutions was measured (pH meter 510, XS instruments) (Table 1).

### 2.3 Gel formation

In order to assess their thermo-sensitivity at 37ºC, the C/GP blank solutions obtained (Table 1) were placed inside a plastic syringe, conveniently cut and isolated with a rubber cap and Parafilm®. The syringe was then emerged in a temperature-controlled water bath at 37ºC (±1°C). The solutions were left there for 20 min in order to make a preliminary assessment of their gelation behavior.

### 2.4 Gelation time of C/GP blank solutions

Gelation time of C/GP blank solutions was studied using the inverted tube test method, according to the methodology described by Gupta and co-workers [28]. The inverted tube test was performed with the solutions that exhibited gel formation in 20 min with the previous method (Table 2). Two mL chromatographic glass tubes were thermo-stabilized in a temperature-controlled bath at 37ºC

(±1°C). Five hundred µL of the sample solution were placed into the tubes and incubated in the bath.

At predetermined time intervals of 30 sec, the tubes were taken out of the water bath and horizontally inverted in order to verify the solution flowability. If the solution did not flow within 15 sec, the time is recorded as gelation time. Inverted tube tests were carried out immediately after the preparation of the solutions, which were then stored at 4ºC. New measurements were taken the day after the preparation and every week through 3 weeks, in order to evaluate the solution stability and the possible changes of the gelation time over that period.

### 2.5 Preparation of formulations and determination of their gelation time

ICG was incorporated in the C/GP solutions; composition is reported in Table 2. About 5 mg of ICG were dissolved in each C/GP solution (20 mL) under stirring condition at 4°C. Gelation time of formulations was determined following the inverted tube test method previously reported. The rationale was the assessment of the dye influence in the gelling properties of these thermosensitive fluids. Inverted tube tests were performed considering the same time intervals carried out for C/GP blank solutions.

### 2.6 Biodegradability

The leader solutions and formulations, that exhibited the best gelation time were selected for further studies and named as reported in Table 3.

Biodegradability studies were conducted following the method of Zang and co-workers[29]. Hydrogels formed from blank solutions and formulations were prepared at 0.6 $cm^3$ volume and 1 cm diameter and immersed in 2 mL of DMEM medium with 0.1% sodium azide containing 1.91 µg/mL chicken egg white lysozyme. Samples were placed in incubator thermostabilized at 37°C for

14 days. The medium was replenished every week of storage. Dried weights of the samples were measured on the 1st, 4th, 7th and 14th days of incubation. Degradation was determined by percentage of weight loss [29].

## 2.7 Rheological characterization

Leader solutions (Table 3) and their corresponding hydrogels were analyzed by rheological methods. The gelling and rheological properties were performed with a Physica MCR101 rheometer (Anton Paar, Austria). The measuring system was parallel-plate type (diameter 50 mm, gap 0.2 mm). Each type of rheological measurement was performed immediately after the preparation of solutions and after 1 week of storage at 4°C and 20°C. Data were expressed as mean ±SD (n = 3).

### 2.7.1 Viscosity measurements

Viscosity measurements of solutions were carried out at 4°C applying a shear rate from 0 to 100 1/s. For all curves the slope (n) was determined in order to evaluate the changes of the viscosity increasing the shear rate.

### 2.7.2 Frequency sweep measurements

Dynamic frequency sweep tests were performed at constant temperature (37°C) and strain (1%) in the limit of the linear viscoelastic region. The storage (G'),and loss moduli (G'') damping factors were determined for angular frequencies (ω) between 0.1 and 100 1/s. The viscoelastic behavior on the hydrogels was analyzed via their corresponding damping factors (tan(δ)) at ω = 10 1/s.

### 2.7.3 Gelation time performed with rheometer

Gelation time was determined at 37°C at a constant angular frequency (ω) of 1.0 1/s at a constant strain of 1 % measuring the storage modulus (G') and loss modulus (G'') as a function of time.

Gelation time of the samples was established at the time of the intersection of G' and G'', where tanδ=1. The differences between gelation time values gained by rheometer and inverted tube test were assessed.

### 2.8 In vitro dye release studies

Each formulation (Table 3) was filled in a dialysis bag previously activated with ethylene diamine tetra-acetic acid (EDTA). The molecular weight cut off (MWCO) of the dialysis bag was 12,000-14,000 and higher than the molecular weight of the dye. The dye release was studied by using the USP dissolution apparatus (DT70, Erweka GmbH, Germany). Each dialysis bag was fixed to the rotating bar of the dissolution tester and lowered into the dissolution vessel containing 900 mL of phosphate buffer (PBS) at pH = 6.5, 37°C (±1°C). The rotation speed of the dialysis bag was 100rpm. Dissolution test was performed up to 16 h. At each prefixed time point, the medium (1mL) was removed for analysis and it was replaced with the corresponding volume of fresh PBS. The samples removed from the medium were immediately analyzed spectrophotometrically (λ= 779 nm) (ThermoSpectronic, Helios, UK). The dissolution studies were conducted in triplicate (mean values are reported). The dye contents of the samples were measured from reference Absorption-Concentration curve of the dye that was constructed by using standard solutions of known ICG concentration in PBS. The same test was performed filling 10 mg of ICG in aqueous solution in another dialysis bag in order to make a comparison with the release behavior of C/GP systems loaded with ICG.

### 2.9 Dye uptake from a preformed hydrogel

The eventual ability of blank hydrogels to up-take ICG dispersed in the liver was investigated filling a preformed blank hydrogel (C1.6/GP15) into a solution of known ICG concentration (0.01

mg/mL) in PBS pH=6.5, 37°C (±1°C). The variation of ICG concentration in the medium was analyzed via UV spectrophotometer (λ= 779 nm) (ThermoSpectronic, Helios, UK) removing samples (1mL) from the medium at 15 min, 30 min, 45 min, 60 min and 90 min. The medium removed for analysis was always replaced with the corresponding volume of fresh PBS.

### 2.10 Ex vivo embolization procedure

Ex vivo studies were carried out on a bovine liver (weight of about 8 kg), thermostabilized at 37°C in a saline bath. The experiments were carried out in standard conditions, with the organ preserved outside of the body. It was flushed at a low pressure saline solution (NaCl 0.9%) and immersed into about 10-15 cm of $H_2O$.

The leader formulations were selected for these studies (Table 3).

The hepatic artery was surgically exposed and then catheterized with a catheter (CVC 14 Gauge). Successively, 5 mL of formulation was slowly injected till a predetermined area of the organ through the distal branches of the hepatic artery (in the right lateral lobe) to selectively embolize an area of 3-4 $cm^2$. Selective visualization of the injection site with a near-infrared (NIR) fluorescence imaging system (PDE; Hamamatsu Photonics K.K. Hamamatsu, Japan) and intraoperative ultrasound (Flexfocus 800, BK medical) were performed in order to assess the localization and gelation of the solutions and the occlusion of the artery. Our group has previously described the combined use of ICG fluorescence and ultrasounds as a useful combine technique to detect small nodules into a liver [16]. In this experiment the probe could allow to confirm the site of gelation shown by fluorescence detection. The site visualized by PDE was then cut open in order to evaluate the hydrogel formation.

## 3. Results

### 3.1 Preparation of C/GP blank solutions and gel formation

Twenty-two C/GP blank solutions, characterized by different C/GP weight ratios were prepared (Table 1). Solutions with the highest concentrations of GP (12-18% w/v) were clear solutions at 4°C when polyol salt was dropwise added. On the contrary, solutions with the lowest concentration of GP (3.0-7.0 % w/v), showed a different behavior at 4°C: the formation under stirring of a milky suspension was observed, whereas a gel-like milky precipitate formed without stirring. However, by shaking or intense stirring, the milky suspension was again obtained.

Gelation of the solutions was assessed through their incubation in a plastic syringe inside a thermo-stabilized bath (37ºC±1°C) and left there for 20 min. Solutions which displayed gelation within that time interval are showed in Table 2. An increase in the hydrogel compactness was found by rising the concentration of C and GP. For the same amount of C, hydrogels with higher amounts of GP were more opaque and they presented a stronger milk coloration, which was in conformity with the observations reported by Ahmadi and co-workers [30].

### 3.2 Gelation time of C/GP blank solutions and formulations

Figure 1 shows gel set in the inverted tube of a formulation chosen as example.

Gelation time results following the inverted tube test method are presented in Table 2. After the preparation, solutions with 2% of C showed increase of gelation time as the GP concentration decreases from 6 min (12% w/v) to 18 min (5% w/v). When C concentration is lowered to 1.6%, higher GP concentrations are necessary to obtain more rapid gelation time: 2 min (18% w/v) and 3 min (15% w/v) were gained.

A decrease in the gelation time values taken one day after the preparation was observed for 2% C solutions with the lowest amount of GP (5.0-7.0%) till 7-3 min, respectively; this behavior was

observed also along the time as a further remarkable decrease in the gelation time from the first to the third week was observed.

The incorporation of ICG into C/GP blank solutions did not display any significant change in the gelation rates of these systems (Table 2). Even after 3 weeks of storage at 4° C, all of the C/GP solutions analyzed, remained temperature-sensitive.

### 3.3 Biodegradability

Figure 2 shows the degradation rate of blank hydrogels or containing ICG. The degradation rate was independent of dye loading and decreased as the C concentration in the solution increased. Over the 14 days of degradation, formulations with 2% C concentration were degraded no more than 54%, whereas formulations with 1.6% C concentration exhibited a degradation rate higher than 60% (Figure 2b). Nevertheless, the cross-link density between C and GP did not affect the degradation rate in case of formulations with 2% C concentration. The only exception was formulation C2/GP7d that exhibited the lowest degradation rate despite the lowest concentration of GP (lowest cross-link density between C and GP). As concerning 1.6% C concentration, formulation degradation rate increased as the cross-link density decreased.

### 3.4 Rheological characterization

#### 3.4.1 Viscosity measurements

For all solutions, viscosity curve was determined at 4°C. In this type of diagram, viscosity is plotted versus shear rate in order to get information about the flow behavior of polymer solutions. Figure 3 shows viscosity of C1.6/GP18, chosen as example. This formulation exhibited a shear-thinning behavior showing viscosity decreases when the shear rate has increased. Furthermore, the storage

time and temperature had also an effect on the viscosity. Other solutions displayed similar viscosity performance.

Data in Table 4 show the viscosity values at the shear rate of 100 1/s. Solutions with high cross-link density between C and GP (formulation C1.6/GP18 and C1.6/GP 15) exhibited an increase of the viscosity during the storage, as already reported in literature [31].

For all viscosity curves, the slope (n) was determined. Table 4 shows that the solution with the lowest cross-link density between C and GP (C2/GP7) exhibited the highest value of n. Solutions with the highest cross-link density (formulation C1.6/GP18 and C1.6/GP15) displayed the lowest values of n as it was expected. The slopes were quite independent from storage temperature (data not shown).

### 3.4.2 Frequency sweep measurements

Figure 4 displays the frequency dependency of G' of hydrogels. High gel strengths (high G') were obtained increasing the cross-link density between C and GP. The only exception was solution C2/GP7 that exhibited a good gel structure despite the lowest cross-link density. Data in Table 5 show the damping factor of hydrogels at angular frequency (ω) of 10 1/s. The lowest values of tan (δ) are related to solutions with the highest molar ratio GP/C. This tendency was general at 4°C and 20°C. The tan (δ) slightly changed during the storage time (at 4°C and 20°C) except for C2/GP7 whose tan (δ) was similar and even lower than tan (δ) plotted for C2/GP10 and C2/GP12, made with the same concentration of C but with higher concentration of GP.

### 3.4.3 Gelation time performed with rheometer

The dynamic viscoelastic functions G' and G'' were measured as a function of time at 37°C. Gelation time ($t_g$) is defined as the crossing point between storage and loss modulus. Figure 5 shows the changes of the storage and the loss modulus as a function of time at 37°C of C1.6/GP18, chosen as example. The gelation point of the samples was established at the intersection of G' and G''.

Values of $t_g$ of all samples extrapolated from sol-gel transitions versus time curves (data not shown), are quite similar to gelation time values carried out with inverted tube test. Thus, there was a good correspondence between the two methodologies.

For C2/GP7, it was not possible to identify the crossing point, and consequently the $t_g$ because G' was always higher than G'' during the time.

From G' versus time curves (Figure 6), the gelation speed of the samples necessary to reach an adequate gel structure can be evaluated, through the slopes of those curves (Table 6). The slopes were dependent on the cross-link density between C and GP and on C and GP concentrations. The only exception was C2/GP7 that exhibited a rapid gelling despite the lowest cross-link density between C and GP.

### 3.5 In vitro dye release studies

Release of ICG from hydrogels into PBS at 37°C over the course of 16 h was measured spectrophotometrically. The results are displayed in Figure 7. The dye in aqueous solution was able to diffuse across the membrane. On the contrary, no significant release of ICG from C1.6/GP15d hydrogel occurred. Indeed, ICG cross through the cut off of the dialysis bag neither in the first minutes when formulation was still in solution, nor when it gelled. No difference in release profile was found in case of other formulations.

### 3.6 Dye uptake from preformed hydrogel

Considering the results from in vitro release studies, which showed the ability of hydrogels to retain ICG, the present test was done to confirm the strong affinity between ICG and hydrogels. A preformed hydrogel (C1.6/GP15) was immersed into PBS solution of known ICG concentration (Figure 8a); the variation of ICG concentration was measured spectrophotometrically at different

time intervals. It was observed a loss of dye absorbance in PBS solution just only after 15 min from 0.952 to 0.294 and decreased till 0.092 after 60 min. (Figure 8b). The observed loss of dye absorbance could be correlated with the strong interaction between C and ICG [32]. As the hydration of C1.6/GP15 hydrogel occurs, an interaction between chitosan and the dye could be hypotized: in fact, green gelled clots were observed suspended into PBS solution which appeared decolored (Figure 8c).

### 3.7 Ex vivo embolization procedure

The injection of the leader formulations (Table 3) through the hepatic artery was performed as previously described. Considering the results gained from the inverted tube test, C2/GP7d was injected the day after the preparation in order to achieve a faster gelation inside the artery.

In all cases the formation of a stable gelled clot was macroscopically observed at the site of embolization in the hepatic parenchyma, due to the rapid gelation of the injected solution, containing the thermosensitive polymer. In this set of experiments, the hydrogel was apparently completely stabilized after 1-5 min at 37°C. The same clot was evident at PDE examination (Figure 9). Furthermore, sections of the liver in correspondence of the injected site confirmed the presence of the gelled clot (Figure 10).

## 4. Discussion

C/GP solutions were prepared to develop a class of ICG-loaded injectable hydrogels, whose potential application is the loco-regional detection and treatment of HCC nodules. Particularly, the solution should be injected down a catheter, which is selectively placed into the arterial branches of a predetermined liver area, similarly to the technique used for superselective TACE. The polymeric compound should be delivered close to the tumor and saturate its vessels. The sol-gel transition

should be fast enough to allow a saturation of the microcirculation. These solutions should be able to exhibit an adequate viscosity to be injected and gelation behavior at physiological temperature (about 37°C). The formed gel should have suitable viscosity to embolize and avoid that hydrogel fragments can flow in the blood circulation. Any peripheral escape of the dye should not be observed.

Most of the solutions prepared are characterized by low concentrations of GP, ranging from 3 to 7% w/v (Table 1); in spite of its endovenous use being approved by the Food and Drug Administration, certain GP toxicity issues have been arisen: after gelation GP starts diffusing out of the physically cross-linked network, resulting in a linear increase of the extraction medium osmolality which results in possible local cytotoxic effects [33]. Therefore the rationale was the preparation of in situ gelling solutions containing the minimum GP amount. In C/GP systems three types of interactions may be involved in the gelation process: (1) hydrogen bonding between C chains, as a consequence of reduced electrostatic repulsion after neutralization with GP; (2) electrostatic attraction between C ammonium groups and GP phosphate groups; (3) C-C hydrophobic interactions [25,34]. Although sol-gel phase transition is driven by hydrophobic interactions, gelation would not occur without mechanisms (1) and (2). This explains the role of pH in the temperature-controlled gelation of C/GP aqueous systems [25]. At low temperatures, C/GP solutions with a pH around 7 do not immediately turn into a gel suggesting that repulsive forces between the C chains are stabilized at low temperatures and destabilized at high temperatures. Ruel-Gariépy and co-workers [35] hypothesized that GP prevents or slows down gelation at low temperature. In fact, polyols are known to stabilize several compounds in aqueous solutions, promoting the formation of a shield of water around some macromolecules in polyol-water mixtures [36]. Accordingly, the presence of GP into C solution promotes the protective hydration of C chains, preventing at low temperatures their association and consequently gelation. C chain hydration is then dependent on the amount of GP added to C solution. If GP concentration is too low, as in the solutions prepared, the formation of a water shield around C chains and their neutralization is only partial, preventing just part of their association and

leading to a gel-like precipitate at low temperatures. The gel-like precipitate formation at 4°C is reversible. At 4°C hydrogen bonding between C-C and C-water are predominant and there is not enough energy for hydrophobic bonds to be established, resulting in a reversible gelation process. Gelation time values obtained immediately after the preparation of the final solutions (Table 2) are in accordance with the results reported by Chenite [25]. In order to achieve a physiologically acceptable pH range and fast gelation at 37ºC, high concentrations of C and GP are required. As a consequence, gelation time increased with the decreasing of GP and C amounts. The increase of the gelation rate observed for solutions with the lowest amount of GP (5.0-7.0%) during the storage, at 4ºC, could be explained in the following way: as we previously reported, low proportions of GP lead to a reversible gelation of C solutions at low temperature even if the pH of the formulations is neutral. Although the hydrogels turned back into a solution under stirring, the presence of small gel nucleus dispersed into the C/GP solutions was observed. As a result, shear stress allows the breaking of the gel network and the formation of small gel nucleus of C/GP which are suspended in aqueous solution. Gel nucleus can aid and accelerate the final gelation induced by temperature through a mechanism of nucleation and growth. The small increase in the gelation rate for the formulations with the highest GP concentrations after 3 weeks of storage was also dependent on the high deacetylation degree of C used for the preparation of these formulations. The combination of high deacetylation degree with high GP concentration leads to high cross-link density between the phosphate groups of GP and the ammonium groups of C [34].

Although all solutions and formulations (Table 2) gel at body temperature, the solutions that exhibited slow gelation cannot be considered suitable for local treatment of HCC as embolic agents. C/GP solution should form a gel quickly in order to provide good occlusion of blood flow [37]. The viscosity and compactness of the corresponding hydrogels that strictly depend on C and GP concentrations, could be further critical parameters [36]. High viscosity may help to control injection, to avoid dilution of the solution and to limit the possibility of migration into collateral arteries [31]. In the latter case, if the arterial blood flow disperses the embolic agent,

cardiopulmonary embolism may occur [38-42]. However, too fast gelation may be problematic because it could determine catheter occlusion. Accordingly, five leader solutions and formulations were selected for further in vitro and ex vivo studies (Table 3). By virtue of the high viscosity, high compactness and adequate gelation rate, these formulations are supposed to remain in the injection site, filling and gelling in vessel cavities. In all cases, formulations remained easily injectable through (CVC 14 Gauge) catheters. Data in Table 4 show the viscosity values at the shear rate of 100 1/s in order to make a comparison with the high shear rate evolving during a hypothetical injection of our solutions. Thus, it is possible to evaluate the injectability of these systems immediately after the preparation and after 1 week of storage. These systems could be considered still injectable, nevertheless an increase of the viscosity during the storage was observed for solutions with high cross-link density between C and GP. The determination of the slope (n) of viscosity curves is a useful approach to understand the resistance to flow of our solutions and consequently the injectability of such systems. The high slope determines low resistance to flow, which indicates a good injectability for these pseudoplastic liquids and, in terms of applicability, a good fit to the desired blood vessel or body cavity. As shown in Table 4 the solution with the lowest cross-link density between C and GP (C2/GP7) exhibits the best injectability despite the formation of a gel-like precipitate at 4°C. This because the gel-like precipitate structure is quite easy to be destroyed during the injection procedure.

Frequency sweep tests were used to characterize the final gel-structure of the five solutions at body temperature. The gels can be described as systems in which the storage moduli (G') are higher than the loss moduli (G'') and/or they are relatively independent from frequency. Lapasin and Pricl [43] classified gels into two classes: strong gels, where the moduli are relatively independent from frequency and weak gels, where the moduli are slightly dependent from frequency. Frequency sweep measurements were carried out in the limit of the linear viscoelastic range, in order to evaluate the frequency dependency of the storage and loss modulus. The high gel strengths (high G') showed by solutions with high cross-link density between C and GP were in conformity with

the results previously reported in literature [35]. The unexpected result of C2/GP7, which exhibited a good gel structure despite the lowest cross-link density, could be explained with the presence of the gel-like precipitation at 4°C. The gel-like precipitate can aid the reaching of a strong gel structure thanks to a nucleation mechanism.

The damping factor reveals the ratio of the viscous and the elastic portion of the viscoelastic deformation behavior. In the hydrogel field, the determination of this value is an important criteria to assess gel formation and hardening process. Therefore, tan (δ) > 1 defines the liquid state and tan (δ) <1 defines the gel state. Furthermore, tan (δ) indicates the elasticity property of the hydrogels: The low tan (δ) determines strong gel structure and, as a consequence, good gel resistance and stability inside the desired tissue, organ, or body cavity.

Data in Table 5 show that the lowest values of tan (δ) are related with solutions with the highest molar ratio GP/C, due to a better neutralization of C chains that leads to an improvement of the interactions involved in the gelation process (hydrogen bonding and hydrophobic interactions). The unexpected tan (δ) of C2/GP7 displayed during the storage time (at 4°C and 20°C), could be explained by the nucleation growth mechanism previously supposed. As previously reported, it was not possible to extrapolate the $t_g$ from sol-gel transitions versus time curves for C2/GP7: G' was always higher than G'' during the time. This comportment is probably due to the presence of the gel-like precipitation at 4°C that leads to an elastic response of the material and that is stronger than the viscous response. As described before, low proportions of GP lead to a reversible gelation of C solutions at low temperature.

The unexpected result for formulation C2/GP7 is found and it is in contrast with the theories reported in literature [25,35]. C2/GP7 exhibited a rapid gelling despite the lowest cross-link density between C and GP. This performance could be explained by the gel-like precipitation at 4 °C. For the other solutions, the slopes are dependent on the cross-link density between C and GP and on C and GP concentrations as we expected.

The degradation rate of C/GP hydrogels with lower concentration of C were faster than those with higher concentrations of this polymer. This behavior was in accordance with previous studies [29,44]. As concerning as the cross-link density, literature reports that hydrogels with high cross-link density have strong gel intensity prohibiting enzyme permeation and causing less degradation [44,45]. However, our results demonstrated that C concentration mainly affects degradation rate as C1.6/GP15d and C1.6/GP18d (although they have high cross-link density) showed higher weight loss compared to 2% C formulations. It can be attribute to the susceptibility of C toward lysozyme [46]. The lowest degradation rate observed for formulation with the lowest cross-link density (C2/GP7d) was also supported by our frequency sweep experiments. This hydrogel exhibited a good gel structure that can be attributed to the nucleation growth mechanism previously mentioned.

The release of ICG from formulations analyzed was not significant. This behavior could be due to an electrostatic interaction between C and ICG [32]. In aqueous solution, the dye is negatively charged thanks to its sulphonic groups, while C is cationic. Therefore, the molecular weight of the ionic complex is bigger than cut off of dialysis membrane used in our release study and ICG is not quantified in the dissolution medium.

A final consideration must be done about the sterilization of these systems: the formulations described in this preliminary work are not sterile because the kind of experiments performed (in vitro and ex vivo) does not require sterile systems. Literature shows that steam sterilization of chitosan may have different effects depending on whether sterilization was performed during its dry state or after it was in solution. Results show that autoclaving the dry chitosan power had no effect on viscosity and thus chitosan dry after sterilization does not undergo any structural changing. Thus, sterile hydrogel can be obtained by treating the dry material and working in aseptic environment [29].

At the current point of this research, we have demonstrated that a polymeric platform can be loaded with a dye to mark a liver area. Considering the results gained from the ex vivo procedure, these in situ gelled C/GP formulations have the potential to remain in correspondence of the injected site for

a long period of time. As we reported before, the time of gelation of these hydrogels was a matter of second, and the process starts immediately at contact with the warmth of blood resulting in a embolization effect of the tumor. Such approach could stop the growth and shrink the tumor burden, while leaving on site a marker, to help the following intraoperative detection of the cancer. At the same time, the removal of the fluorescent tissue would be guided throughout the operation by a real time observation of the parenchymal margins. The final result could be a better outcome for the patients, with an advantage offered by the pre-treatment of the tumor and a resulting aid during the resection. However, this preliminary study is a "proof of concept" and its clinical use still requires further experiments.

## 5 Conclusions

Thermosensitive chitosan/glycerophosphate platforms were prepared and loaded with indocyanine green, which did not interfere with their gelation process. C2/GP7d thanks to a gel-like precipitation, rapidly forms in situ compact gels and represents a good candidate for filling vessels. Taking into consideration the obtained results, formulations could be injected through a catheter into tumor nodules; as the solution gels in these areas, a prolonged visualization of these nodules can be achieved in "real time imaging" during the embolization and the following hepatic resection of HCC.

## Acknowledgements

The project is supported by the European Union and co-financed by the European Social Fund TAMOP-4.2.2.A-11/1/KONV-2012-0035.

## Declaration of interest

The authors state no conflict of interest regarding this manuscript.

**References**

[1] Ferenci P, Fried M, Labrecque D, et al. Hepatocellular carcinoma (HCC): a global perspective. J ClinGastroenterol 2010;44:239-45 ** An exhaustive review about Hepatocellular carcinoma.

[2] Tam KY, Leung KC, Wang YX. Chemoembolization agents for cancer treatment. Eur J Pharm Sci 2011;44:1-10

[3] Giunchedi P, Maestri M, Gavini E, et al. Transarterial chemoembolization of hepatocellular carcinoma. Agents and drugs: an overview. Part 1. Expert Opin Drug Deliv 2013;10:679-90 * An overview regarding embolization treatments in cancer therapy.

[4] Breedos C, Young G. The blood supply of neoplasms in the liver. Am J Pathol 1954;30:969-77

[5] Kemeny NE, Niedzwiecki D, Hollis DR, et al. Hepatic Arterial Infusion Versus Systemic Therapy for Hepatic Metastases From Colorectal Cancer: A Randomized Trial of Efficacy, Quality of Life, and Molecular Markers (CALGB 9481). J Clin Oncol 2006;24:1395-1403

[6] Raoul JL, Heresbach D, Bretagne JF, et al. Chemoembolization of hepatocellular carcinomas. A study of the biodistribution and pharmacokinetics of doxorubicin. Cancer 1992;70:585-90

[7] Laurent A. Microspheres and nonspherical particles for embolization. Tech Vasc Interv Radiol 2007;10:248-56

[8] Giunchedi P, Maestri M, Gavini E, et al. Transarterial chemoembolization of hepatocellular carcinoma. Agents and drugs: an overview. Part 2. Expert Opin Drug Deliv 2013;10:799-810 * An overview regarding embolization treatments in cancer therapy.

[9] Lewis AL, Gonzalez MV, Lloyd AW, et al. DC Bead: in vitro characterization of a drug-delivery device for Transarterial Chemoembolization. J Vasc Interv Radiol 2006;17:335-42 * A nice paper that clearly describes TACE with DC Bead.

[10] Landsman ML, Kwant G, Mook G. A, et al. Light-absorbing properties, stability, and spectral stabilization of indocyanine green. J Appl Physiol 1976;40:575-83

[11] Gotoh H, Yamada T, Ishikawa O, et al. A Novel Image-Guided Surgery of Hepatocellular Carcinoma by Indocyanine Green Fluorescence Imaging Navigation. J Surg Oncol 2009;100:75-79

[12] Ishizawa T, Fukushima N, Shibahara J, et al. Real-time identification of liver cancers by using indocyanine green fluorescent imaging. Cancer 2009;115:2491-504

[13] Kokudo N, Ishizawa T. Clinical application of fluorescence imaging of liver cancer using indocyanine green. Liver Cancer. 2012;1:15-21

[14] Ishizawa T, Masuda K, Urano Y, et al. Mechanistic background and clinical applications of indocyanine green fluorescence imaging of hepatocellular carcinoma. Ann Surg Oncol. 2014;21:440-48.

[15] Alacam B, Yazici B, Intes X, et al. Extended Kalman filtering for the modeling and analysis of ICG pharmacokinetics in cancerous tumors using NIR optical methods. IEEE Trans Biomed Eng 2006;53:1861-71

[16] Peloso A, Franchi E, Canepa MC, et al. Combined use of intraoperative ultrasound and indocyanine green fluorescence imaging to detect liver metastases from colorectal cancer. H P B 2013;15: 928-34

[17] Unno N, Inuzuka K, Suzuki M, et al. Preliminary experience with a novel fluorescence lymphography using indocyanine green in patients with secondary lymphedema. J Vasc Surg 2007;45:1016-21

[18] Qiu Y, Park K. Environment-sensitive hydrogels for drug delivery. Adv Drug Deliv Rev 2001;53:321-39

[19] Klouda L, Mikos AG. Thermoresponsive hydrogels in biomedical applications. Eur J Pharm Biopharm 2008;68:34-45 ** An interesting paper that describes potential applications of thermosensitive hydrogels in the medical field.

[20] Wang J, Pang Q, Liu Z, et al. A New Liquid Agent for Endovascular Embolization: Initial Clinical Experience. ASAIO J 2009;55:494-97

[21] Weng LN, Zantek ND, Rostamzadeh P, et al. An in situ forming biodegradable hydrogel-based embolic agent for interventional therapies. Acta Biomater 2013;9:8182-91

[22] Muzzarelli RAA. Human enzymatic activities related to the therapeutic administration of chitin derivatives. Cell Mol Life Sci 1997;53:131-40 * An important review that describes the potential importace of chitosan in the pharmaceutical field.

[23] Hirano S, Seino H, Akiyama Y, et al. Chitosan: a biocompatible material for oral and intravenous administrations. Prog Biomed Polym: Springer US, 1990;283-90

[24] Rassu G, Gavini E, Mattana A, et al. Improvement of antiamoebic activity of rokitamycin loaded in chitosan microspheres. The Open Drug Deliv J 2008;2:38-43

[25] Chenite A, Chaput C, Wand D, et al. Novel injectable neutral solutions of biodegradable gels in situ. Biomaterials 2000;1:2155-61 * A nice paper that describes the use of chitosan and glycerol phosphate for the preparation of gels.

[26] Chenite A, Buschmann MD, Wang D, et al. Rheological characterisation of thermogelling chitosan / glycerol-phosphate solutions. Carbohydr Polym 2001;46:39-47

[27] Kashyap A, Viswanad B, Sharma G, et al. Design and evaluation of biodegradable, biosensitive in-situ gelling system for pulsatile delivery of insulin. Biomaterials 2007;28:2051-60

[28] Gupta D, Tator CH, Shoichet MS. Fast-gelling injectable blend of hyaluronan and methylcellulose for intrathecal, localized delivery to the injured spinal cord. Biomaterials 2006;27:2370-79

[29] Zang S, Dong G, Peng B, et al. A comparison of physicochemical properties of sterilized chitosan hydrogel and its applicability in a canine model of periodontal regeneration. Carbohydr Polym 2014;113:240–48

[30] Ahmadi R, De Bruijn JD. Biocompatibility and gelation of chitosan-glycerol phosphate hydrogels. J Biomed Mat 2007;86A:824-32

[31] Ruel-Gariépy E, Leclair G, Hildgen P, et al. Thermosensitive chitosan-based hydrogel containing liposomes for the delivery of hydrophilic molecules. J Control. Release 2002;82:373-83 * An interesting paper describing thermosensitive formulations designed for injection.

[32] Wu H, Zhao H, Song X, et al. Self-assembly-induced near-infrared fluorescence nanoprobes for effective tumor molecular imaging. J Mater Chem B 2014;2:5302-08

[33] Jauhari S, Dash AK. A mucoadhesive in situ gel delivery system for paclitaxel. AAPS PharmSciTech, 2006;7:154-59

[34] Zhou HY, Chen XG, Kong M, et al. Preparation of chitosan-based thermosensitive hydrogels for drug delivery. J Applied Polym Sci 2009;112:1509-15

[35] Ruel-Gariépy E, Chenite A, Chaput C, et al. Characterization of thermosensitive chitosan gels for the sustained delivery of drugs. Int J Pharm 2000;203:89-98

[36] Back JF, Oakenfull D, Smith MB. Increased thermal stability of proteins in the presence of sugars and polyols. Biochemistry 1979;18:5191-96

[37] Coutu JM, Fatimi A, Berrahmoune S, et al. A new radiopaque embolizing agent for the treatment of endoleaks after endovascular repair: Influence of contrast agent on chitosan thermogel properties. J Biomed Mater Res 2013;101B:153-161

[38] Khan I, Vasudevan V, Nallagatla S, et al. Acute lung injury following transcatheter hepatic arterial chemoembolization of doxorubicin-loaded LC beads in a patient with hepatocellular carcinoma. Lung India 2012;29:169-72

[39] Wu JJ, Chao M, Zhang GQ, et al. Pulmonary and cerebral lipiodol embolism after transcatheter arterial chemoembolization in hepatocellular carcinoma. World J Gastroenterol 2009;15:633-35 * Interesting research paper describing possible embolism after TACE.

[40] Shiah HS, Liu TW, Chen LT, et al. Pulmonary embolism after transcatheterarterial chemoembolization. Eur J Cancer Care 2005;14:440-42

[41] Naorungroj T, Naksanguan T, Chinthammitr Y. Pulmonary lipiodol embolism after transcatheter arterial chemoembolization for hepatocellular carcinoma: a case report and literature review. J Med Assoc Thai 2013;96:270-75

[42] Zhao H, Wang HQ, Fan, QQ, et al. Rare pulmonary and cerebral complications after transarterial chemoembolisation for hepatocellular carcinoma: a case report. World J Gastroenterol 2008;14:6425-27

[43] Lapasin R, Pricl S. Rheology of Industrial Polysaccharides: Theory and Applications. London: 1995

[44] Ganji F, Abdekhodaie MJ, Ramazani ASA. Gelation time and degradation rate of chitosan-based injectable hydrogel. J Sol-Gel Sci Tech 2007;42:47–53

[45] Dang QF, Yan JQ, Li JJ, et al. Controlled gelation temperature, pore diameter and degradation of a highly porous chitosan-based hydrogel. Carbohydr Polym 2011;63:171-78

[46] Drury JL, Mooney DJ. Hydrogels for tissue engineering: scaffold design variables and applications. Biomaterials 2003;24:4337-51

**Table 1.** Composition and pH of C/GP blank solutions prepared for the evaluation of gel formation

| C (% w/v) | GP (% w/v) | pH |
|---|---|---|
| 2.0 | 12.0 | 7.31 |
| 2.0 | 10.0 | 7.25 |
| 2.0 | 7.0 | 7.21 |
| 2.0 | 6.0 | 7.17 |
| 2.0 | 5.0 | 6.98 |
| 2.0 | 4.0 | 6.98 |
| 2.0 | 3.5 | 6.95 |
| 2.0 | 3.0 | 6.95 |
| 1.6 | 18.0 | 7.42 |
| 1.6 | 15.0 | 7.34 |
| 1.5 | 7.0 | 7.29 |
| 1.5 | 6.0 | 6.98 |
| 1.5 | 5.0 | 6.96 |
| 1.5 | 4.0 | 6.96 |
| 1.5 | 3.5 | 6.85 |
| 1.5 | 3.0 | 6.81 |
| 1.0 | 7.0 | 6.89 |
| 1.0 | 6.0 | 6.88 |
| 1.0 | 5.0 | 6.86 |
| 1.0 | 4.0 | 6.84 |
| 1.0 | 3.5 | 6.80 |
| 1.0 | 3.0 | 6.80 |

**Table 2.** Composition and gelation time of C/GP blank solutions (S) and formulations (F) performed with inverted tube test

| composition | | Gelation time (min:s) | | | | | | | | | |
|---|---|---|---|---|---|---|---|---|---|---|---|
| C | GP | after prep. | | 1 day | | 1 week | | 2 weeks | | 3 weeks | |
| (%w/v) | (%w/v) | S | F | S | F | S | F | S | F | S | F |
| 2.0 | 12.0 | 06:00 | 06:00 | 06:00 | 06:30 | 06:00 | 06:00 | 05:30 | 05:30 | 05:00 | 05:30 |
| 2.0 | 10.0 | 07:00 | 07:00 | 07:00 | 07:00 | 07:00 | 07:30 | 04:30 | 04:30 | 04:00 | 04:00 |
| 2.0 | 7.0 | 14:00 | 14:30 | 03:00 | 03:00 | 02:00 | 02:30 | 01:30 | 01:30 | 01:00 | 01:00 |
| 2.0 | 6.0 | 16:30 | 16:00 | 04:30 | 05:00 | 01:00 | 01:00 | 00:30 | 00:30 | 00:30 | 00:30 |
| 2.0 | 5.0 | 18:00 | 18:00 | 07:30 | 07:30 | 00:30 | 01:00 | 00:30 | 00:30 | 00:30 | 01:00 |
| 1.6 | 18.0 | 02:00 | 02:00 | 02:00 | 02:00 | 02:00 | 02:00 | 02:00 | 02:00 | 01:30 | 01:30 |
| 1.6 | 15.0 | 03:00 | 03:00 | 03:00 | 03:00 | 03:00 | 02:30 | 03:00 | 03:00 | 02:30 | 02:30 |

**Table 3.** Composition of leader solutions and formulations

| Code | C (% w/v) | GP (% w/v) | ICG (% w/v) |
|---|---|---|---|
| C2/GP12 | 2.0 | 12.0 | - |
| C2/GP12d | 2.0 | 12.0 | 25 |
| C2/GP10 | 2.0 | 10.0 | - |
| C2/GP10d | 2.0 | 10.0 | 25 |
| C2/GP7 | 2.0 | 7.0 | - |
| C2/GP7d | 2.0 | 7.0 | 25 |
| C1.6/GP18 | 1.6 | 18.0 | - |
| C1.6/GP18d | 1.6 | 18.0 | 25 |
| C1.6/GP15 | 1.6 | 15.0 | - |
| C1.6/GP15d | 1.6 | 15.0 | 25 |

**Table 4.** Viscosity, η, at shear rate of 100 1/s of solutions stored at 4°C and 20°C. Data were expressed as mean ± SD (n = 3)

| Solution | η (Pa × s) | | | Slopes (n) after preparation |
|---|---|---|---|---|
| | Storage at 4°C | | Storage at 20°C | |
| | after preparation | 1 week | 1 week | |
| C2/GP12 | 0.476 ± 0.06 | 0.412 ± 0.05 | 1.040 ± 0.07 | 0.379 ± 0.09 |
| C2/GP10 | 0.358 ± 0.03 | 0.302 ± 0.08 | 0.710 ± 0.10 | 0.333 ± 0.08 |
| C2/GP7 | 0.205 ± 0.02 | 0.370 ± 0.03 | 0.152 ± 0.03 | 1.163 ± 0.10 |
| C1.6/GP18 | 0.157 ± 0.02 | 0.244 ± 0.03 | 0.317 ± 0.05 | 0.125 ± 0.01 |
| C1.6/GP15 | 0.160 ± 0.01 | 0.274 ± 0.03 | 0.270 ± 0.07 | 0.129 ± 0.01 |

**Table 5**. Damping factors (tan (δ)) at 10 1/s of hydrogels, obtained from solutions stored at 4°C and 20°C. Data were expressed as mean ± SD (n = 3)

| | tan (δ) | | |
|---|---|---|---|
| Solution | Storage at 4°C | | Storage at 20°C |
| | after preparation | 1 week | 1 week |
| C2/GP12 | 0.28 ± 0.01 | 0.29 ± 0.02 | 0.26 ± 0.01 |
| C2/GP10 | 0.29 ± 0.03 | 0.30 ± 0.01 | 0.28 ± 0.01 |
| C2/GP7 | 0.30 ± 0.03 | 0.27 ± 0.02 | 0.24 ± 0.01 |
| C1.6/GP18 | 0.19 ± 0.02 | 0.17 ± 0.03 | 0.16 ± 0.04 |
| C1.6/GP15 | 0.22 ± 0.03 | 0.24 ± 0.03 | 0.22 ± 0.03 |

**Table 6.** Slopes (n) of G' versus time curves of solutions after preparation. Data were expressed as mean ±SD (n = 3)

| Solution | Slope (n) |
|---|---|
| C2/GP12 | 21.75 ± 6.53 |
| C2/GP10 | 13.80 ± 4.00 |
| C2/GP7 | 47.70 ± 4.31 |
| C1.6/GP18 | 16.80 ± 2.11 |
| C1.6/GP15 | 6.84 ± 1.05 |

## Figure captions

**Figure 1.** Photographs of the gelation process observed by inverted tube test. Formulation is a flowable liquid at room temperature (A) and it is transformed to a rigid hydrogel at 37°C (B).

**Figure 2.** Degradation of hydrogel obtained from blank solutions (A) and formulations (B) over 14 days. Data are depicted as mean ± SD (n = 3).

**Figure 3.** Viscosity curves of C1.6/GP18, chosen as example, after preparation and after 1 week of storage at 4°C and 20°C.

**Figure 4.** Frequency dependence of hydrogels after preparation.

**Figure 5.** Sol-gel transitions versus time of C1.6/GP18 at 37°C after preparation, chosen as example.

**Figure 6.** Comparison of the slopes of solutions after preparation.

**Figure 7.** *In vitro* release profile of ICG from C1.6/GP15d, chosen as example, compared with that of diffusion from ICG water solution. Data were expressed as mean ± SD (n = 3).

**Figure 8.** Absorbance curve of ICG solution versus time during dye uptake from preformed hydrogel; picture of ICG solution immediately after the immersion of C1.6/GP15 hydrogel (A) and after 90 min (B).

Figure 9. Selective visualization of the injection site with a near-infrared fluorescence imaging system PDE. The embolizing formulation was injected through the hepatic artery in the right lateral lobe. The figure shows the bright fluorescence of ICG under the infrared PDE camera and its neat localization into the injection site. The dotted line indicates the limit of the organ.

Figure 10. Section of the liver after the in situ gelation of C1.6/GP15d. The picture demonstrates gelled clots at the site of injection after cutting open the area previously localized by PDE and showed in Figure 9.

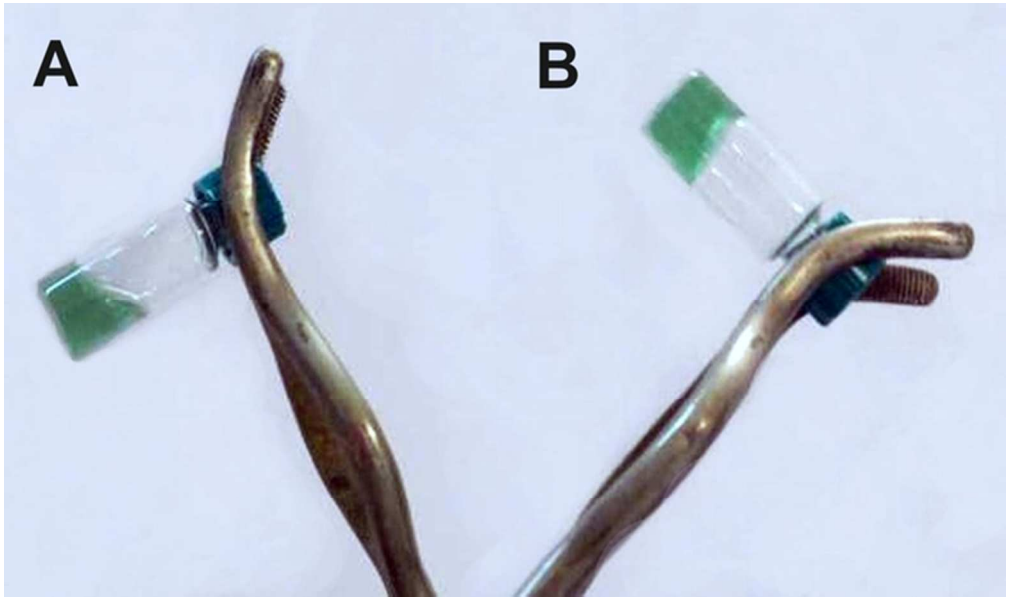


Figure 1. Photographs of the gelation process observed by inverted tube test. Formulation is a flowable liquid at room temperature (A) and it is transformed to a rigid hydrogel at 37°C (B).
59x35mm (300 x 300 DPI)

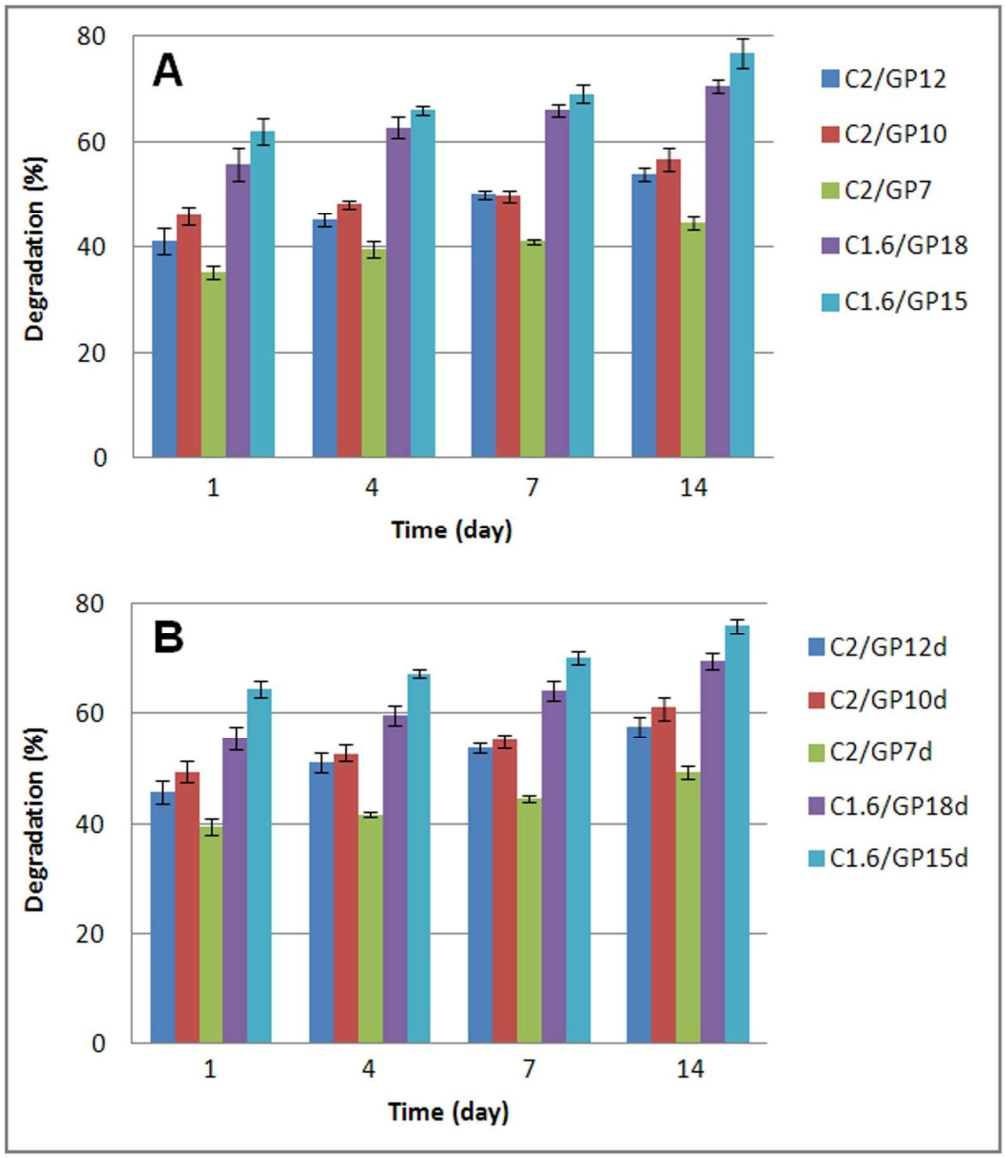


Figure 2. Degradation of hydrogel obtained from blank solutions (A) and formulations (B) over 14 days. Data are depicted as mean ± SD (n = 3).
115x132mm (300 x 300 DPI)

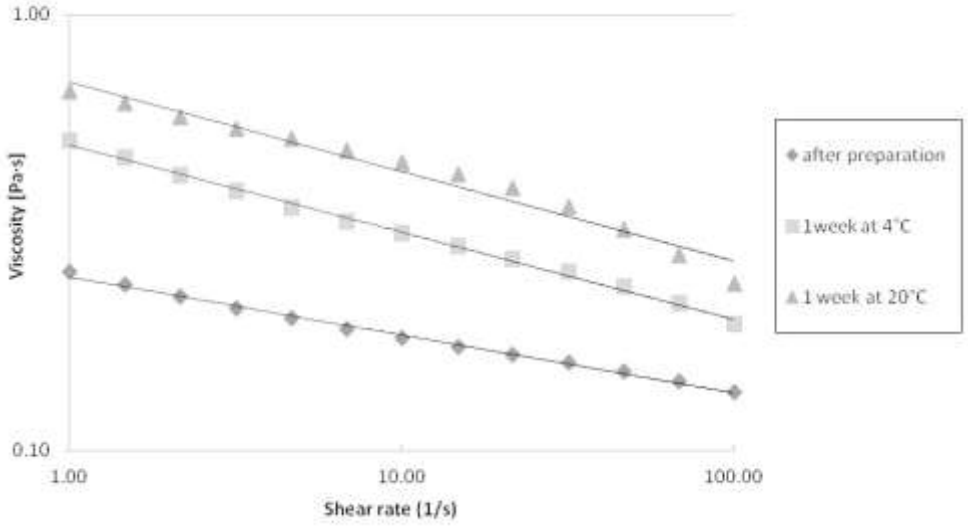


Figure 3. Viscosity curves of C1.6/GP18, chosen as example, after preparation and after 1 week of storage at 4°C and 20°C.
171x100mm (150 x 150 DPI)

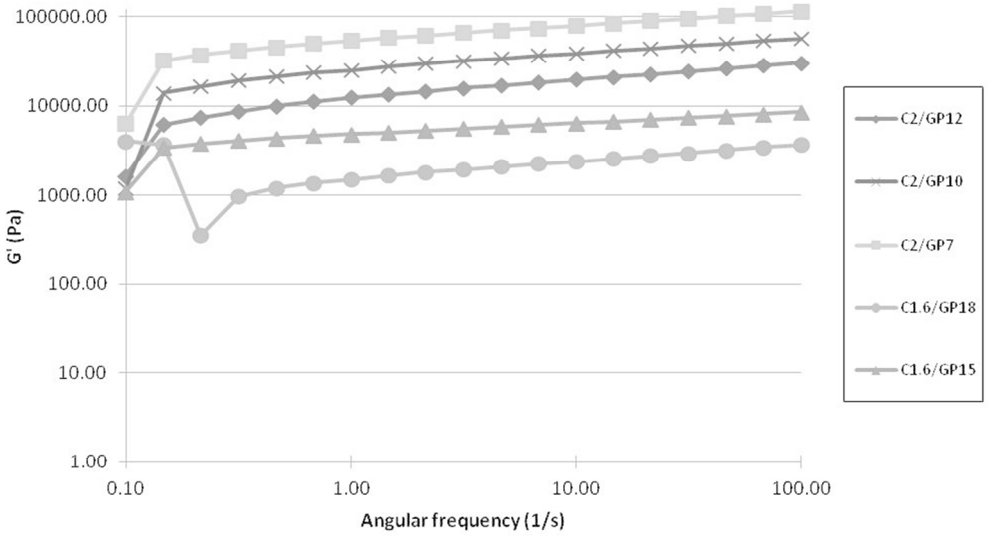


Figure 4. Frequency dependence of hydrogels after preparation.
169x101mm (150 x 150 DPI)

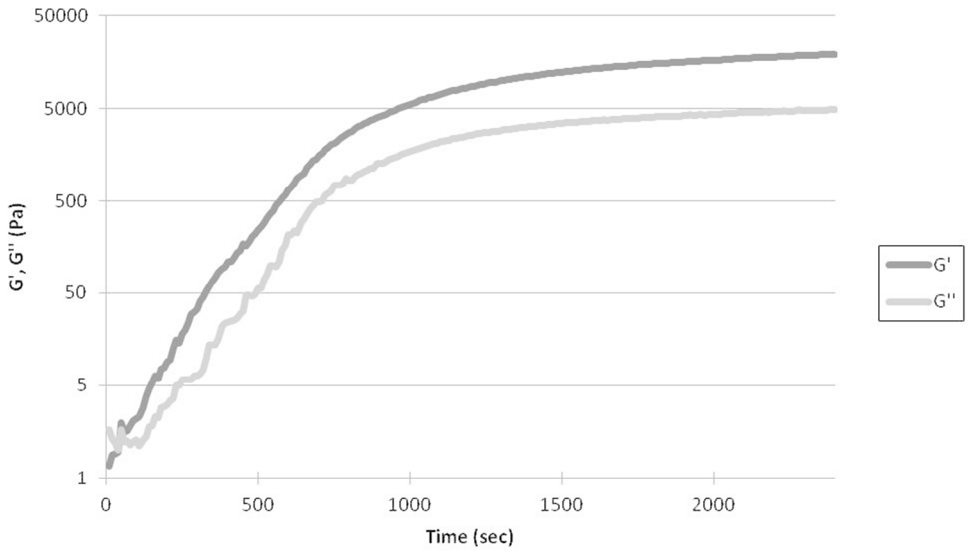


Figure 5. Sol-gel transitions versus time of C1.6/GP18 at 37°C after preparation, chosen as example.
169x99mm (150 x 150 DPI)

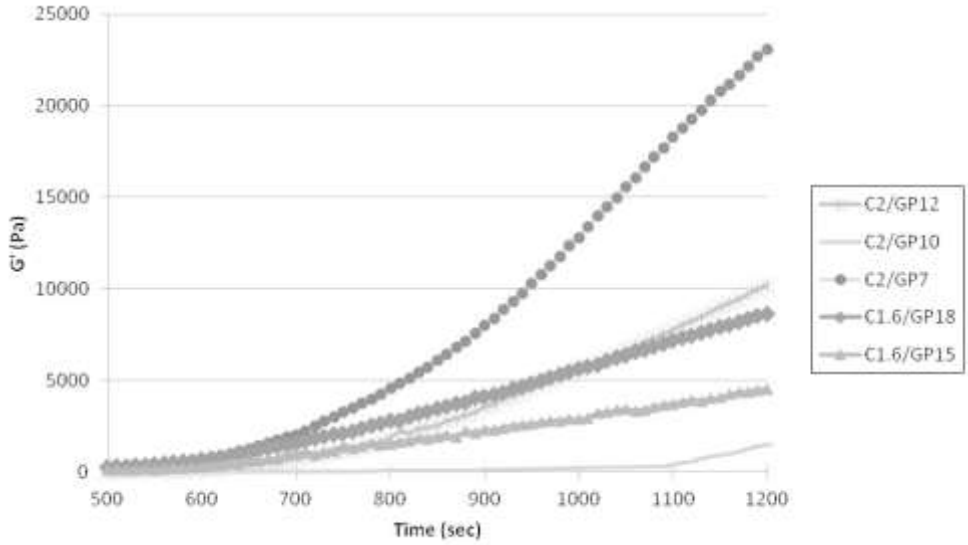


Figure 6. Comparison of the slopes of solutions after preparation.
170x98mm (150 x 150 DPI)

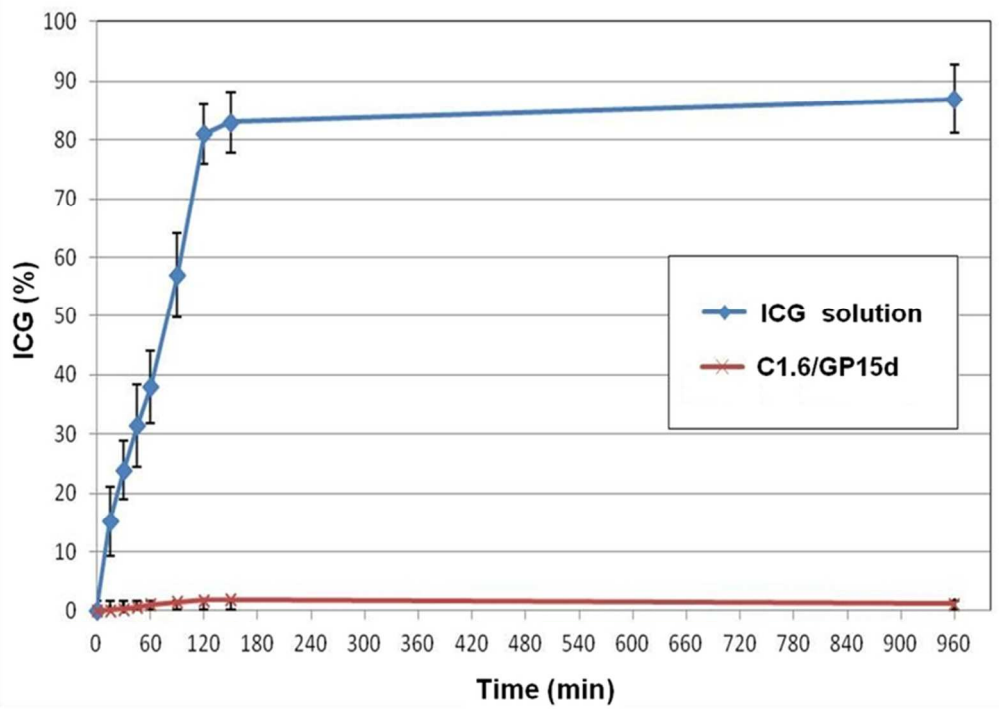


Figure 7. In vitro release profile of ICG from C1.6/GP15d, chosen as example, compared with that of diffusion from ICG water solution. Data were expressed as mean ± SD (n = 3).
72x52mm (300 x 300 DPI)

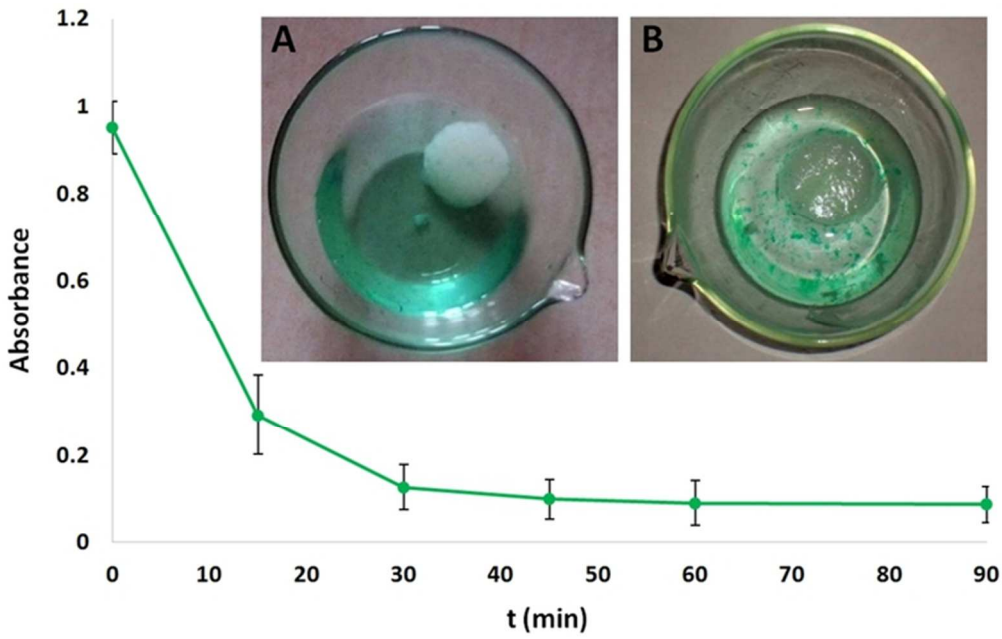


Figure 8. Absorbance curve of ICG solution versus time during dye uptake from preformed hydrogel; picture of ICG solution immediately after the immersion of C1.6/GP15 hydrogel (A) and after 90 min (B).
63x40mm (300 x 300 DPI)

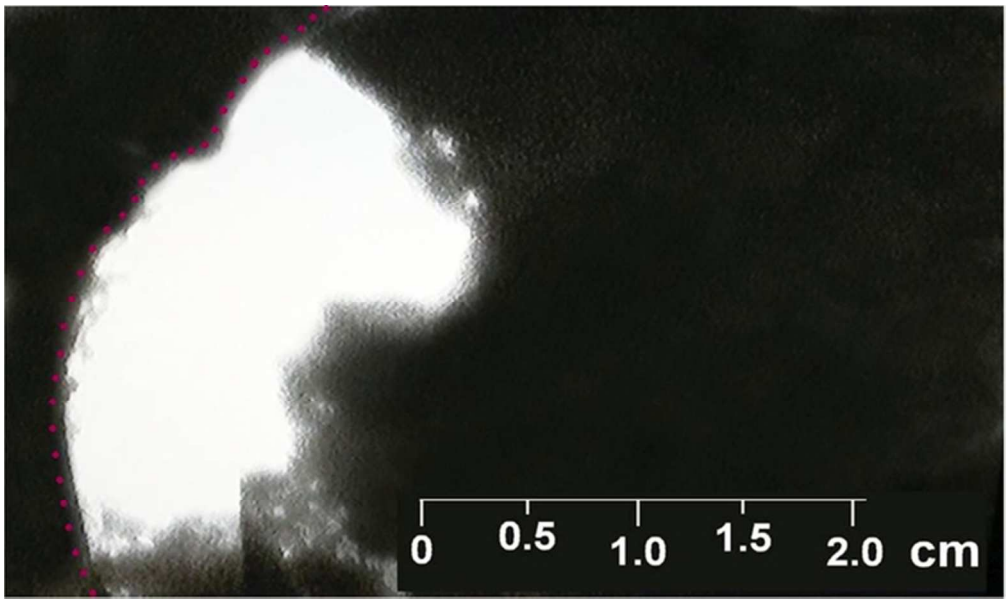


Figure 9. Selective visualization of the injection site with a near-infrared fluorescence imaging system PDE. The embolizing formulation was injected through the hepatic artery in the right lateral lobe. The figure shows the bright fluorescence of ICG under the infrared PDE camera and its neat localization into the injection site. The dotted line indicates the limit of the organ.
59x35mm (300 x 300 DPI)

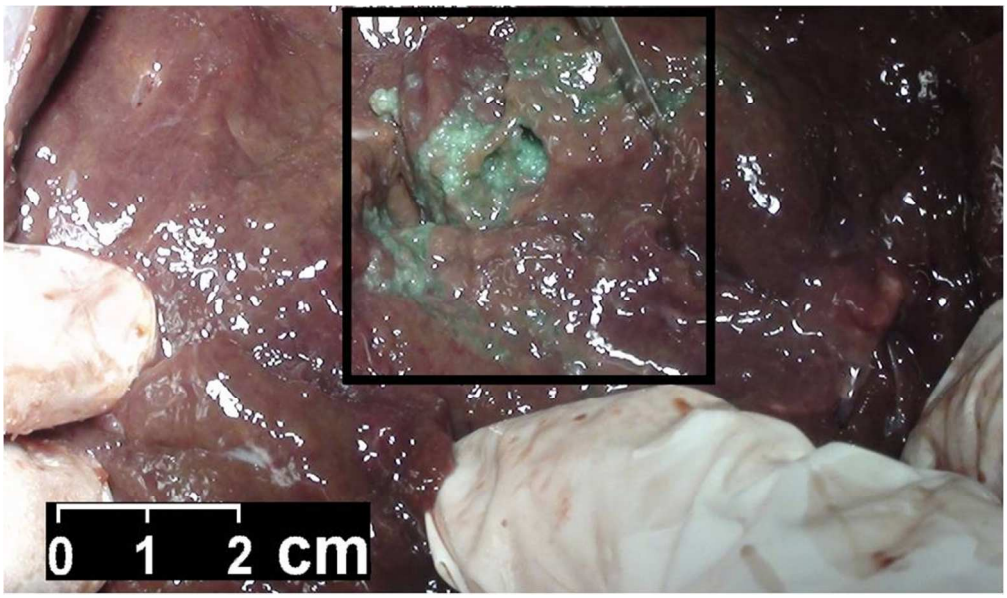


Figure 10. Section of the liver after the in situ gelation of C1.6/GP15d. The picture demonstrates gelled clots at the site of injection after cutting open the area previously localized by PDE and showed in Figure 9.
170x100mm (150 x 150 DPI)

Expert Opinion on Drug Delivery - **ID EODD-2015-0040**

**Title:** Development of thermosensitive chitosan/glicerophospate injectable in situ gelling solutions for potential application in intraoperative fluorescence imaging and local therapy of hepatocellular carcinoma: a preliminary study

We would like to express our appreciation for the Reviewers of our manuscript. We have revised the manuscript according to the suggestion of Reviewer 1. The modified portions of the revised manuscript are indicated in blue type.
We hope that all these changes will satisfy the Reviewers and the Editor.

Reviewer comments

Referee: 1

I thank the authors for addressing my comments and I think the paper is much better. There remains a few errors in the introduction regarding the commercial products. I would suggest replacing the sentences from page 3, lines 27 to 43 with the following paragraph to ensure accuracy of the information:

"Briefly, there are microspheres available on the market for so called “bland” embolization or transarterial embolization (TAE). These include Bead Block®, Embospheres®, Embozene® and Contour SE®. DC Bead® was designed to load therapeutic agents to enable one-step transarterial chemoembolization (TACE) and consists of polyvinyl alcohol (PVA) hydrogel modified with sulfonate groups that were first to demonstrate the ability to load and release chemotherapeutics in a controlled manner- a concept known as a drug-eluting bead (DEB). Other DEB systems are also now commercially available but based on microspheres with carboxylic acid functionality instead (HepaSphere® and Tandem®)."

*Authors: the paragraph has been modified as referee’s suggestion.*

Referee: 2
The manuscript has been revised according to all Reviewers comments and is now acceptable for publication.